Increasing Accuracy of Discrete-Time Computation of Linear Rheological and Viscoelastic Material Functions

VAIRIS SHTRAUSS
Institute for Material Mechanics
University of Latvia
23 Aizkraukles Street, LV 1006 Riga
LATVIA
strauss@pmi.lv

Abstract: - The paper is addressed to increasing the accuracy of discrete-time computation of linear rheological and viscoelastic material functions belonging to the class of smooth non-bandlimited (NBL) signals. It is demonstrated that the ideology of classical discrete-time processing, which is based on preserving accurate spectrum over the Nyquist frequency band, ignores the anti-aliasing distortion caused by removal of a signal portion above the Nyquist frequency needed for preserving accurate spectrum and, so, gives the inadequate accuracy evaluation of computed material functions. To ensure the adequate accuracy evaluation of NBL material functions, we propose to waive the criterion of preserving accurate spectrum over the Nyquist frequency band, but instead to use the criterion of maintaining accurate shape of a material function in the time-domain. Both the criteria are compared and the appropriate error models are developed and investigated. Increase of accuracy of filtering algorithms is studied for computing NBL material functions. Design of discrete-time filters is proposed by the identification method with employing bandlimited input and output portions of a pair of NBL functions. The proposed design approach is validated by constructing a discrete-time differentiator with employing bandlimited portions of the Cauchy pulse and its derivative.

Key-Words: - Linear Rheological and Viscoelastic Material Functions, Discrete-Time Processing, Accuracy, Non-Bandlimitedness, Filtering Algorithms

1 Introduction

Material characterization [1,2], by which a material's structure and properties are evaluated, includes also various transformations of experimental data. A typical example of experimental data transformation is the interconversion between various rheological and viscoelastic material functions [3] needed for evaluation of material properties over long time intervals and wide frequency ranges [4-7], when the possibilities of direct experimentation are limited.

The exact mathematical description of interrelations between various rheological and viscoelastic material functions are known from the linear theory of viscoelasticity [4-7]. The typical experimental data transformations, which are carried out by discrete-time (DT) interconversion [3], include the interconversions between the static and dynamic material functions, and vice versa, the interconversions between the real and imaginary parts of dynamic material functions, the recovery of the relaxation and retardation spectra from various static or dynamic material functions, etc.

Historically, a great number of various methods [8-12] have been derived for computing the rheological and viscoelastic material functions. Nowadays, DT methods are increasingly involved in computing material functions [3]. However, the computation of the rheological and viscoelastic material functions has received little attention in the literature from the standpoint of DT processing [13-15]. In routine practice, the rheological and viscoelastic material functions are often computed by the traditional DT processing focused on processing bandlimited (BL) signals.

There are several aspects of DT processing that are not sufficiently investigated yet and could negatively impact on computation performance of the rheological and viscoelastic material functions, such as:

- the specific monotonic and locally monotonic character and the Fourier/Mellin transforms with

unbounded supports [3] that allow to categorise the rheological and viscoelastic material functions as *smooth non-bandlimited* (NBL) signals;
- the bandlimited processing ideology and accuracy criteria used in the classical DT processing [13] that could be inappropriate for computing NBL material functions;
- DT algorithms that are designed without considering the features of NBL material functions.

The goal of this study was to investigate how to increase computing accuracy of the linear rheological and viscoelastic material functions to take into account the above aspects and to minimise their potential detrimental effects.

The paper is structured as follows. In next Section, the differences between the classical discrete-time processing of continuous-time (CT) signals and discrete-time processing of NBL material functions are disclosed. Section 3 is devoted to modification of DT processing to ensure the adequate accuracy evaluation for computed material functions. Filtering algorithms for computing material functions are considered in Section 4. In Section 5, a design method of DT filters is proposed based on using bandlimited portions of input and output signals. Here, the evaluation results are provided for a designed DT differentiator. Finally, conclusions are given in Section 7.

2 Discrete-Time Processing of NBL Material Functions

2.1 Classical DT Processing of CT Signals

Main features of the classical DT processing of CT signals [13] are as follows: (i) the processing is focused on BL signals or signals that can be forced to be bandlimited; (ii) it carries out the processing that is equivalent to CT one, to achieve this the processing works with CT input and output signals and only their transformation is implemented discretely; (iii) the theoretical foundation of the classical DT processing is the Nyquist theorem [13], according to that a BL processing ideology is realised based on preserving the accurate spectra of signals over the Nyquist frequency band.

A simplified block diagramm of the classical DT processing of CT signals is shown in Fig. 1. A CT input signal is sampled (converted from CT to DT in C/D block) at appropriate sampling frequency (here, angular) $\Omega_S = 2\pi / T$, where T is sampling period. In order to keep all information about the input signal, the sampling frequency should be at least two times greater than the higher frequency of the original CT signal. When it is not possible to guarantee this condition, so-called aliasing distortions arise resulting that the reconstructed signal from samples differs from the original CT signal. To avoid aliasing distortions [13], the spectrum of input signal is limited to the so-called the Nyquist frequency $\Omega_{Ny} = \Omega_S / 2$ by removing frequencies above the Nyquist frequency by analog low-pass anti-aliasing filtering (AAF) at cut-off frequency $\Omega_C = \Omega_{Ny}$ prior sampling. The sampled signal is processed by a DT algorithm and finally is converted back to CT (D/C) output signal.

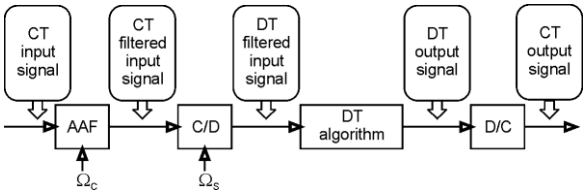

Fig. 1. A block diagram for the classical DT processing of CT signals.

2.2 Features of DT Processing of NBL Material Functions

Two noticeable differences between the classical DT processing [3] and the DT processing of NBL material functions are follows:

(i) as outlined in the Introduction, the rheological and viscoelastic material functions belong to the class of smooth non-bandlimited signals [3,16,17].

(ii) NBL material functions are numerically processed, as a rule, with no conversion of DT result back to the CT domain [3]. For computing NBL material functions, the block diagram (Fig. 1) is used without D/C block.

2.3 Characteristic Time-Domain Portions of a NBL Material Function

The non-bandlimitedness, i.e. the Fourier/Mellin transforms with unbounded supports, allows to represent the spectrum of a NBL material function as one consisting from several frequency bands (Fig. 2) with the corresponding signal portions in the time domain that are discretely processed in different way.

Therefore, the Nyquist frequency Ω_{Ny} divides the infinite spectrum of a NBL material function into a Nyquist frequency band $[-\Omega_{NY}, \Omega_{Ny}]$ and a band

above the Nyquist frequency $|\Omega| > \Omega_{Ny}$ with the corresponding bandlimited portion (BLP) and out-of-band portion (OBP) in the time domain

$$x(t) = x_{BLP}(t) + x_{OBP}(t). \quad (1)$$

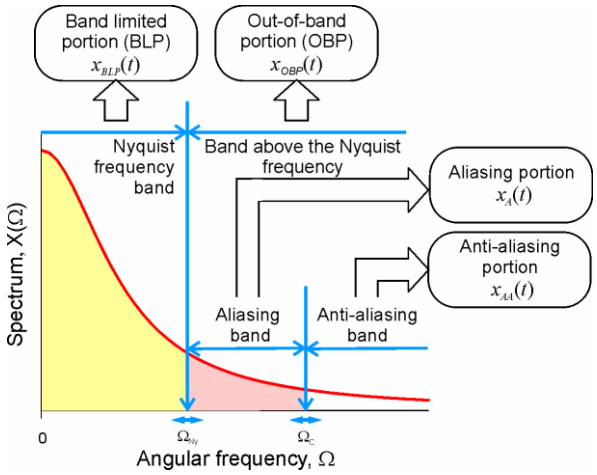

Fig. 2. Decomposition of a NBL material function into characteristic portions.

In its turn, cut-off frequency Ω_C conditionally splits the band above the Nyquist frequency into an aliasing band (Ω_{Ny}, Ω_C] and an anti-aliasing band (Ω_C, ∞) with the characteristic aliasing and anti-aliasing portions in the time domain

$$x_{OBP}(t) = x_A(t) + x_{AA}(t). \quad (2)$$

As it is well known [13-15], only bandlimited portion $x_{BLP}(t)$ is processed in a direct way by the DT algorithm used, whereas aliasing portion $x_A(t)$ is processed as a signal transformed back to the Nyquist frequency band, but anti-aliasing portion $x_{AA}(t)$ is removed by AAF. So, according to (2), OBP determines the common effect from the non-bandlimitedness that manifests in the form of aliasing arrising from processing of aliasing portion $x_A(t)$, and in the form of anti-aliasing arrising from removing anti-aliasing portion $x_{AA}(t)$.

For simplicity, in this study, we consider only the cases with the maximum aliasing/zero anti-aliasing portions and the maximum anti-aliasing/zero aliasing portions corresponding to two idealized extreme processing alternatives:

(i) a *full-band processing* without AAF ($\Omega_C = \infty$), when complete OBP is processed as a signal generated back the Nyquist frequency band; and
(ii) a *processing mode with ideal AAF* with cut-off at the Nyquist frequency ($\Omega_C = \Omega_{Ny}$), when OBP is completely removed.

2.4 A Drawback of Classical DT Processing for NBL Material Functions

According to the classical DT processing ideology, it is common to assume [14] that (i) a signal portion with spectrum above the Nyquist frequency is unwanted so should be removed by AAF, and (ii) the error from AAF is smaller than that caused by aliasing. These assumptions are no longer valid for NBL material functions. Making a NBL material function to be bandlimited is achieved by removal of OBP, which can in no way be considered as unwanted because is a natural component of a NBL material function being essential for its adequate representation and evaluation. As shown in [16,17], a question about whose of aliasing or anti-aliasing error will be higher, depends on how OBP, transformed back to the Nyquist frequency band, will be processed by the DT algorithm used.

So, the main drawback of the classical DT processing for computing NBL material functions is inadequate accuracy evaluation due to ignoring an the essential component – OBP and its caused anti-aliasing distortion.

3 Modification of DT Processing for NBL Material Functions

3.1 Accuracy Criteria

To overcome the above drawback, we propose to waive the frequency-domain accuracy criterion of classical DT processing [13] based on preserving accurate spectrum over the Nyquist frequency band, but instead to use the the time-domain accuracy criterion of maintaining accurate shape of a material function in the time-domain.

The proposal seems to contradict previous studies [13] that emphasize the negative effect of the aliased spectra, but the use the time-domain accuracy criterion is justified by the fact that material functions are discretely processed with no conversion of DT results back to the CT domain (see the second difference in Sub-Section 2.2). If D/C conversion is not caried out, there is no longer the incontrovertible argument for preserving the accurate spectrum of the output signal over the Nyquist frequency band, and other criteria may be used, for example, computation of the samples as accurately as possible against a reference output signal. In fact, the proposal is not original, historically, the time-domain accuracy criteria based on theoretical models have long time been used in processing material functions [3].

Both the accuracy criteria are illustrated in Fig. 3 in example of comparison of CT and DT (sampled) vaveforms and spectra for a NBL test signal so-called Cauchy pulse [16,17]

$$c(t) = 1/(1+t^2) \tag{3}$$

having spectrum

$$C(\Omega) = \pi \exp(-|\Omega|)$$

and the following BLP

$$c_{BLP}(t) = c(t)[1+\exp(-\Omega_{Ny})(t\sin\Omega_{Ny}t - \cos\Omega_{Ny}t)] \tag{4}$$

It can be seen, that theoretically both the time-domain and frequency-domain accuracy criteria can be used, but it is impossible to attain simultaneously accurate shape and spectrum for a sampled NBL function. If accurate time domain waveform $c(t)$ is kept, it has aliased spectrum $C_S(\Omega)$, if exact spectrum $C_{S,BLP}(\Omega)$ is preserved over the Nyquist frequency band, the reconstructed waveform $c_{BLP}(t)$ is distorted by the anti-aliasing distortion.

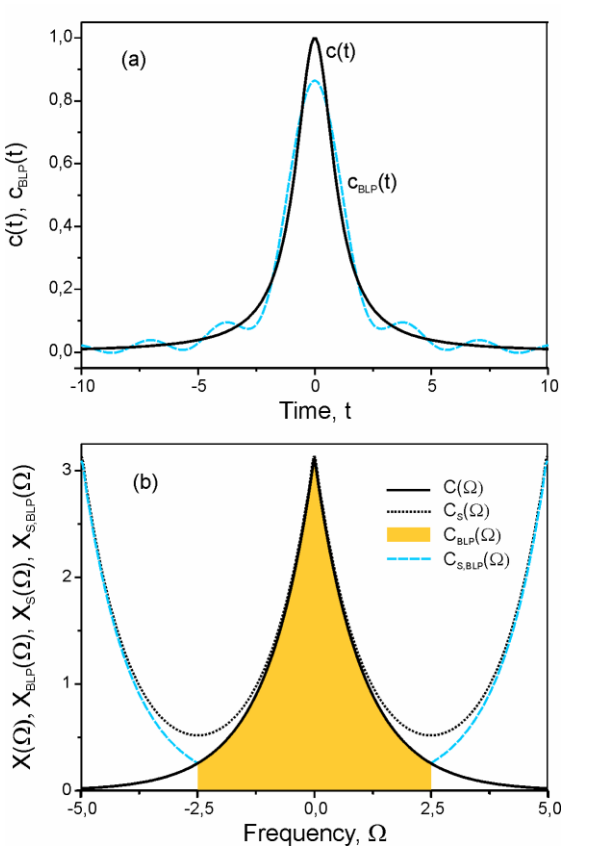

Fig. 3. The Cauchy pulse and its BLP (a) with and the spectra of CT (coloured) and sampled signals (lines) (b) at Ω_{NY} = 2.5.

3.2 Error Models

In this Sub-Section, the error models will be developed and compared for both the frequncy-domain and time-domain accuracy criteria considered in the previous Sub-Section.

Assume that NBL material function (1) has to be discretely transformed into other otput NBL material function

$$y(t) = y_{BLP}(t) + y_{OBP}(t) \tag{5}$$

to compute an estimate for (5). The estimate in the full-band processing mode will be composed from both the estimates of BLP and OBP

$$\hat{y}_{full}(t) = \hat{y}_{BLP}(t) + \hat{y}_{OBP}(t),$$

whereas, in the proccesing mode with ideal AAF with cut-off at the Nyquist frequency, it will consist of single BLP estimate

$$\hat{y}_{AAF}(t) = \hat{y}_{BLP}(t),$$

since OBP of input signal $x_{OBP}(t)$ is completely removed by ideal AAF resulting in $\hat{y}_{OBP}(t) = 0$.

The total time-domain error of the computed output material function $\hat{y}(t)$ is calculated as a difference between the computed function and the appropriate reference function

$$e(t) = \hat{y}(t) - y_{ref}(t). \tag{6}$$

3.2.1 Error Model for Frequency-Domain Accuracy Criterion

The frequency-domain accuracy criterion used in the classical DT processing [13] is based on preserving accurate spectrum over the Nyquist frequency band, which is equivalent to the following reference function in the time domain

$$y_{FD\_ref}(t) = y_{BLP}(t). \tag{7}$$

Eq. (7) allows to interpret the frequency-domain accuracy criterion also as a BL one. In the full-band processing mode, reference function (7), according to (6), gives the following expression for the total error

$$\begin{aligned} e_{FD\_full}(t) &= \hat{y}_{BLP}(t) + \hat{y}_{OBP}(t) - y_{BLP}(t) \\ &= e_{BLP}(t) + \hat{y}_{OBP}(t) \end{aligned}, \tag{8}$$

where the first term of Eq. (8)

$$e_{BLP}(t) = \hat{y}_{BLP}(t) - y_{BLP}(t) \tag{9}$$

represents BLP error, but the computed OBP of output material function $\hat{y}_{OBP}(t)$ is interpreted as a maximum aliasing error,

$$e_{FD\_\max A}(t) = \hat{y}_{OBP}(t).$$

Similarly, in the processing mode with ideal AAF, the total error is equal to

$$e_{FD\_AAF}(t) = e_{BLP}(t). \quad (10)$$

Eq. (10) gives the total error that is equal to BLP error (9) meaning that removing OBP does not affect the total error, which is not in accordance with the physical considerations and, so, is not applicable to NBL material functions.

3.2.2 Error Model for Time-Domain Accuracy Criterion

The proposed time-domain accuracy criterion is equivalent to NBL reference function

$$y_{TD\_ref}(t) = y(t), \quad (11)$$

which allows to interpret the time-domain accuracy criterion as a non-bandlimited one. Reference function (11) according to (6) gives the following total error

$$\begin{aligned} e_{TD\_full}(t) &= \hat{y}_{BLP}(t) + \hat{y}_{OBP}(t) - y_{BLP}(t) - y_{OBP}(t) \\ &= e_{BLP}(t) + e_{OBP}(t) \\ &= e_{BLP}(t) + e_{TD\_\max A}(t) \end{aligned} \quad (12)$$

in the full-band processing mode, and

$$\begin{aligned} e_{TD\_AAF}(t) &= \hat{y}_{BLP}(t) - y_{BLP}(t) - y_{OBP}(t) \\ &= e_{BLP}(t) - y_{OBP}(t) \\ &= e_{BLP}(t) + e_{TD\_\max AA}(t) \end{aligned}, \quad (13)$$

in the processing mode with ideal AAF. Errors (12) and (13) show that, in processing NBL signals, i.e. in computing NBL material functions, there always is a non-bandlimited error, which is limited by the maximum aliasing error equal to the error of computed OBP

$$e_{TD\_\max A}(t) = e_{OBP}(t) = \hat{y}_{OBP}(t) - y_{OBP}(t), \quad (14)$$

and the maximum anti-aliasing error equal to OBP of exact output signal with minus sign

$$e_{TD\_\max AA}(t) = -y_{OBP}(t). \quad (15)$$

3.2.3 Comparison of Errors Models

In Fig. 4, variation of mean square errors (MSEs) with sampling frequency is compared for both the frequency-domain and time-domain accuracy criteria in differentiting of the Cauchy pulse (2) by a 12-point differentiator designed by the impulse response truncation (IRT) method [15]. The differentiation MSE is evaluated as

$$MSE = (1/M)\sum_{m=1}^{M} e^2(t_m), \quad (16)$$

calculated over the predetermined time interval [0, 10] for M = 100 samples for the appropriate time-domain error.

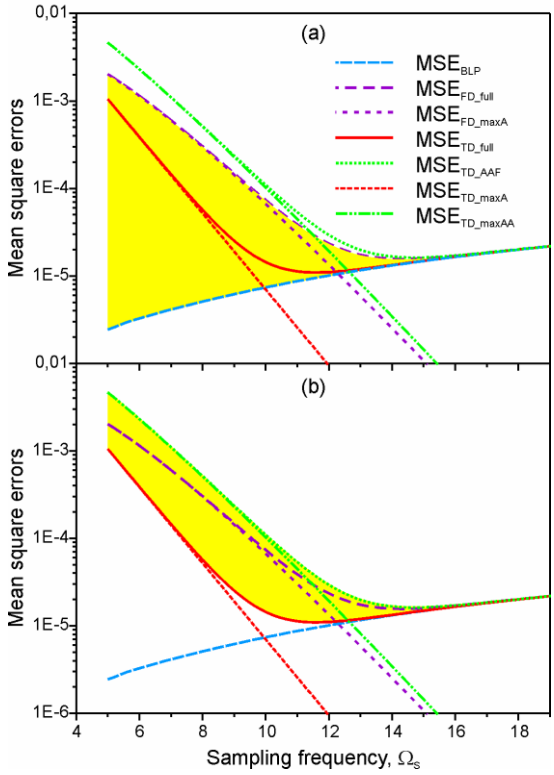

Fig. 4. Variation of differentiation MSEs with sampling frequency for the Cauchy pulse. Coloured area in (a): variation limits of the total MSE for the frequency-domain criterion; coloured area in (b): variation limits of the total MSE for the proposed time-domain criterion.

Total errors for both the accuracy criteria converge to BLP error at high sampling frequencies, however, the errors for both the accuracy criteria differ significantly at low frequencies, particularly, their lower limits. It can be seen that the frequency-domain criterion preserving accurate spectrum over the Nyquist frequency band ignores the anti-aliasing distortion caused by removal of OBP, which reflects as a wrong – zero estimate for the non-

bandlimitedness error in the processing mode with ideal AAF.

4 Filtering Algorithms for Computing Material Functions

Interrelations between the different rheological and viscoelastic material functions are often given in the form of convolution transforms [3]. Since ideal filters are also described by convolution transforms, DT and digital filters are widely used for their computing.

A large amount of examples can be found in literature, where discrete-time (digital) filters have been constructed for computing convolution transforms with the aim to make the computation more effective. The two major areas, where DT filters have been most used for computing integral transforms probably are geophysical electromagnetic prospecting [18-20] and material science [3]. In modern signal processing [13-15,21], a DT differentiator [22] inverting a convolution transform with the step-function kernel, likely, is the most known filter for computing a convolution transform.

In computing convolution transforms, the shapes of convolved waveforms usually carry information, so attainment of accurate as possible waveforms generally is of primary importance. So, design problem of a filter for computing a convolution transform should be formulated in the time domain as finding an impulse response that produces convolved waveforms as accurately as possible under the specific processing conditions (filter's length, sampling frequency, etc.). This design differs from that of conventional frequency selective filters [13-15,21] intended for removing unwanted frequency parts or extracting useful parts of a signal, where filter coefficients must be found to provide some desired frequency response.

Filters designed in the frequency domain usually are not optimal for computing convolution transforms, in the sense that they do not produce maximum accurate convolved waveforms potentially available for the given signal and the filter's length stated at the specified sampling frequency. A main reason of this is a lack of knowledge how the frequency response of a DT filter should deviate from the ideal frequency response to produce a convolved waveforms as accurately as possible. In other words, there are limited possibilities to formulate an optimal design specification in the frequency domain and so to design an optimal filter for computing a convolution transform.

In specific areas, such as geophysical prospecting [18-20] and material science [3], it is widespread to design filters for convolution transforms from a pair of known input-output functions related with each other by the given transform. This approach has been generalized as an identification (ID) method implementing design of filters in the input-output signal domain [23], although it can be also interpreted as a method based on the learning principle [3,24].

An advantage of ID method is that it effectively eliminates various effects, such as data truncation, rounding-off, etc., from which cannot be avoided by the frequency-domain methods. The identification method has been also used for constructing DT algorithms for non-linear – non-convolution transforms, such as computing the real and imaginary parts [25,26] and the relaxation spectrum [27,28] from the magnitude response, where a non-convolution transform is approximated by a convolution transform and computed by a DT filter. A main drawback of the ID method often pointed out in the literature [18-20] is dependence of the filter coefficients on the pair of input and output functions chosen for the identification.

5 Filter Design Based on BLPs of Input and Output Signals

5.1 Idea behind Filter Design

In Fig. 5, typical variations of MSEs with sampling frequency are shown for DT filters designed by different methods, such as already mentioned IRT method [15] and ID method [3,23], as well as the Parks-McClellan (PM) algorithm [13,14,29]. MSEs are computed according to (16) for the time-domain errors corresponding to the time-domain criterion. To simplify the formula, the indices without "TD" is used for "MSE".

It can be seen, that the non-bandlimitedness error (coloured lane), which is limited by the maximum anti-aliasing error (15) and maximum aliasing error (14), practically does not depend on algorithm, at the same time BLP errors are highly algorithm dependent. So, the total computation error of a smooth NBL signal can be practically decreased only by two means: (i) by increasing sampling frequency, and (ii) by improving the computing accuracy for BLP. Thus, a key idea behind the proposed filter design is finding maximum accurate algorithms for computing BLP. To materialize the idea, we propose to design filters in the input-output signal domain by the identification method [3,23] with using pairs of

the bandlimited portions of NBL input and output functions.

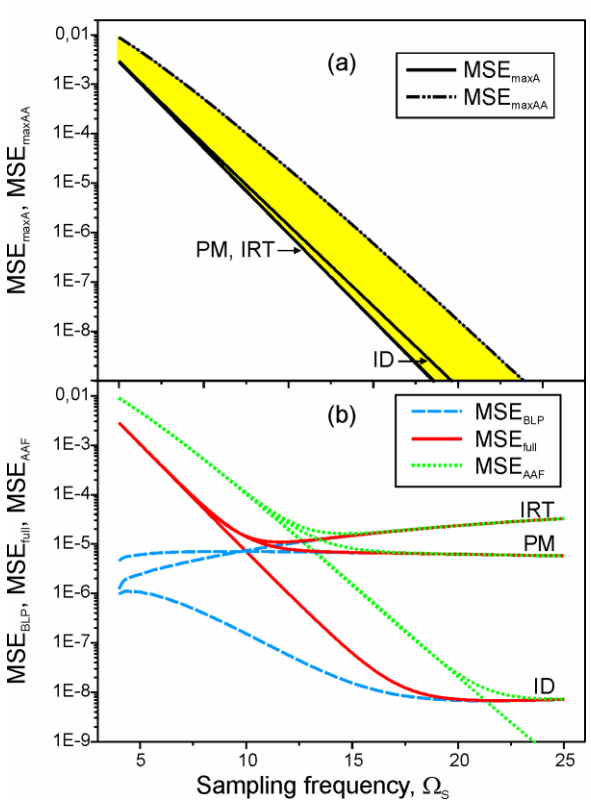

Fig. 5. Variation of differentiation MSEs with sampling frequency for the Cauchy pulse and its characteristic time-domain portions: (a) maximum aliasing and anti-aliasing MSEs, coloured lane – interval of variation of the non-bandlimitedness error; (b) MSEs of BLPs and total MSEs.

5.2 Design Example of Differentiator

In this Sub-section, we demonstrate designing a DT differentiator by using BLP (4) of the Cauchy pulse (3) and BLP

$$\begin{aligned} c'_{BLP}(t) = \\ & c^2(t)[-2t + 2t\exp(-\Omega_{Ny}t)\cos(\Omega_{Ny}t) - \\ & 2t^2\exp(-\Omega_{Ny}t)\sin(\Omega_{Ny}t)] + \\ & c(t)\{\exp(-\Omega_{Ny}t)[\Omega_{Ny}t\cos(\Omega_{Ny}t) + \\ & \sin(\Omega_{Ny}t) + \Omega_{Ny}\sin(\Omega_{Ny}t)]\} \end{aligned} \quad (17)$$

of derivative of the Cauchy pulse

$$c'(t) = -2tc^2(t).$$

The filter coefficients are found for bandlimited input (4) by minimizing time domain error between the differentiator's output $\hat{y}(t)$ and the exact bandlimited derivative (17)

$$e(t) = \hat{y}(t) - c'_{BLP}(t)$$

according to MSE criterion (16).

5.3 Accuracy Evaluation of Designed Differentiator

In Fig. 6, differentiation MSEs of the Cauchy pulse with sampling frequency are shown for 12-point differentiators designed by different methods.

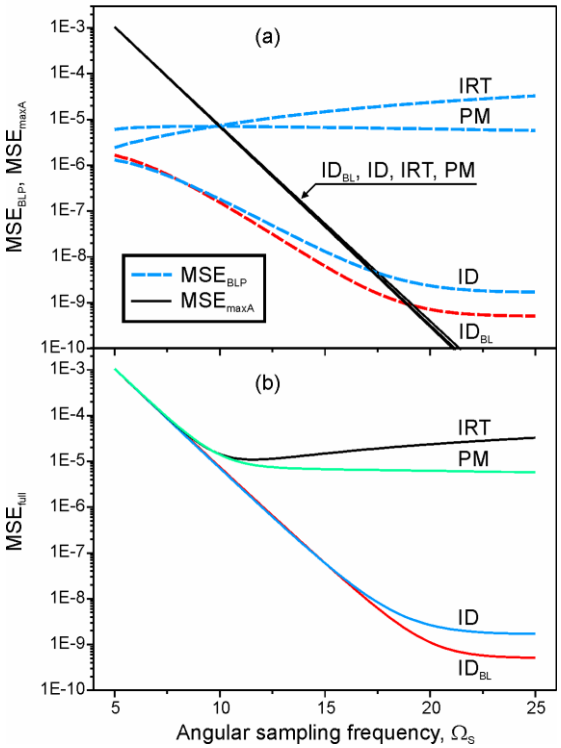

Fig. 6. Variation of differentiation MSEs with sampling frequency for derivatives of the Cauchy pulse: (a) MSEs of BLPs and OBPs, (b) full differentiation MSEs.

It can be seen that the four differentiators have practically equal non-bandlimitedness error (as a limit error in the form of maximum aliasing error MSE_{maxA}) that exponentially decays with sampling frequency. At the same time, the different differentiators exceedingly unlike process BLP producing the error that slightly increases with sampling frequency for IRT differentiator, is practically constant for PM differentiator and decays with sampling frequency for ID and ID_{BL} differentiators. How it was expected, ID_{BL} differentiator has the smallest MSE_{BLP}.

The non-bandlimitedness (maximum aliasing) error is greater than BLP errors at low frequencies resulting in its prevailing contribution in the total errors MSE_{full} for all the differentiators (Fig. 6(b)). Due to the exponentially decaying MSE_{maxA} and the slower decaying MSE_{BLP}, BLP errors overcome the

non-bandlimitedness error at higher sampling frequencies, which are various for different differentiators. Fig. 6 actually witnesses the rightness of the idea behind the proposed design method that the total processing error for smooth NBL signals can be decreased by two means – increasing sampling frequency and improving the processing accuracy of BLPs.

Qualitatively similar behaviour of total MSEs with sampling frequency to that of the Cauchy pulse (see Fig. 6(b)) has been observed for some other smooth NBL test signals, such as the Hilbert transform of the Cauchy pulse (Fig. 7)

$$x(t) = t/(1+t^2)$$

having derivative

$$y(t) = (1-t^2)/(1+t^2)^2,$$

the Gaussian function (Fig. 8)

$$x(t) = \exp(-\pi t^2),$$

having derivative

$$y(t) = -2\pi t \exp(-\pi t^2),$$

and for a bandlimited signal – the unnormalized sinc-function (Fig. 9)

$$x(t) = \mathrm{sinc}(t) = \sin(t)/t$$

having derivative

$$y(t) = \cos(t)/t - \sin(t)/t^2.$$

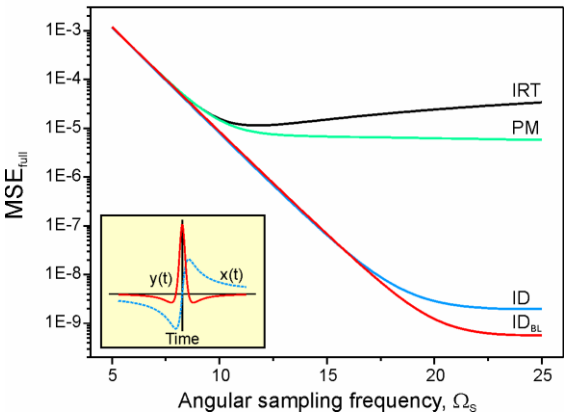

Fig. 7. Variation of total differentiation MSEs with sampling frequency for the Hilbert transform of the Cauchy pulse (small window).

Variation of the differentiation error with sampling frequency for the Hilbert transform of the Cauchy pulse (see Fig. 7) and the Gaussian function (see Fig. 8) shows that the total error is formed from both of components (1) similarly as for the Cauchy pulse (see Fig. 6) with prevailing of MSE_{maxA} at low sampling frequencies and MSE_{BLP} at the higher ones.

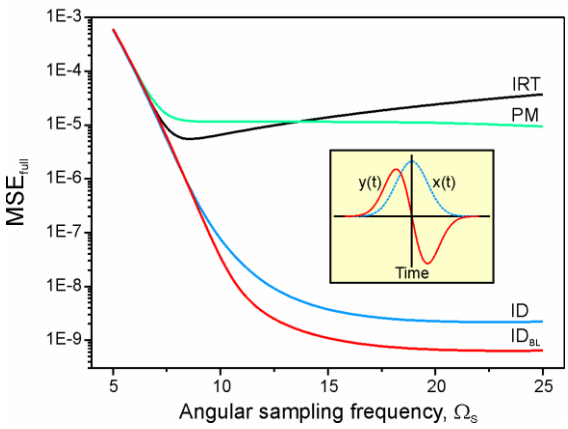

Fig. 8. Variation of total differentiation MSEs with sampling frequency for the Gaussian function (small window).

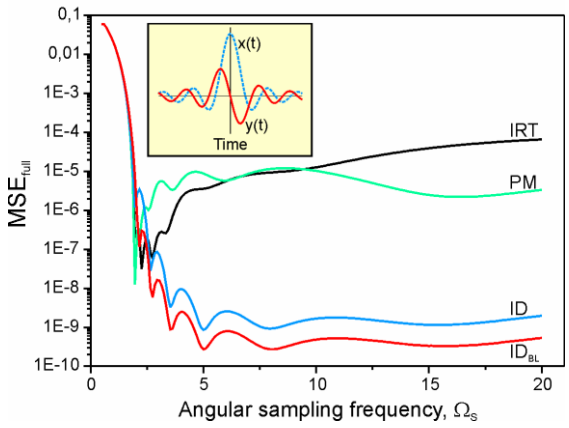

Fig. 9. Variation of total differentiation MSEs with sampling frequency for sinc-function (small window).

For sinc-function (see Fig. 9) as a bandlimited one, we cannot speak about the non-bandlimitedness error, however, here, also OBP appears, when the Nyquist frequency is smaller than the limit frequency of the frequency band with non-zero spectrum. This OBP creates the aliasing error, which as a very fast decaying error is seen in Fig. 9 at low frequencies.

5.4 Magnitude Responses

In Fig. 10, the errors of magnitude responses $|H(j\Omega)| - \Omega$ are compared for the four 12-point differentiators. It can be seen that the deviations of magnitude responses from the ideal magnitude response do not reflect the common differentiation accuracy (see Fig. 6 – Fig. 9). This observation confirms the statement made in the Section 4 that a lack of knowledge about optimal design specification

in the frequency domain limits the frequency-domain design methods to construct accurate DT algorithms for computing convolution transforms.

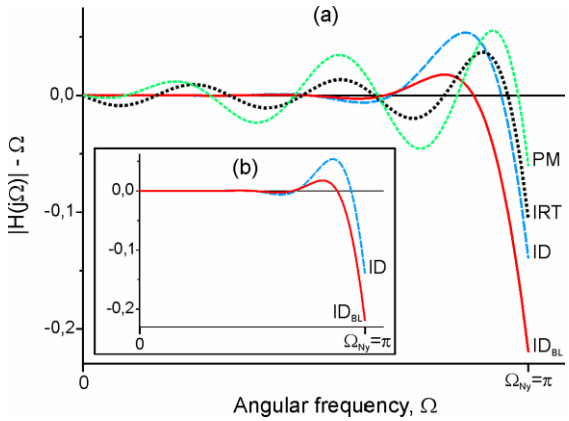

Fig. 10. Errors of magnitude responses for 12-point differentiators: (a) ID_{BL}, ID, PM and IRT differentiators, (b) ID_{BL} and ID differentiators.

Designing FIR filters for computing integral transforms in the specific fields [3,18-20] has shown that smooth magnitude responses are required in the vicinity of zero frequency to compute accurate convolved waveforms. The errors of magnitude responses of ID and ID_{BL} differentiators (Fig. 10 (b)) approve this experience and demonstrate that the more accurate ID_{BL} differentiator (see Fig. 6 – Fig. 9) has the smoother magnitude response than that of the ID differentiator.

7 Conclusion

The paper is addressed to increasing the accuracy of discrete-time computation of linear rheological and viscoelastic material functions with taking into account their belonging to a class of smooth non-bandlimited (NBL) signals. We demonstrate that the ideology of classical discrete-time processing, based on preserving accurate spectrum over the Nyquist frequency band, does not provide the adequate accuracy evaluation for computed material functions, because ignores the anti-aliasing distortion caused by removal of out-of-band portion (OBP) of a NBL material function needed for preserving accurate spectrum over the Nyquist frequency band. To ensure the adequate accuracy evaluation for computed material functions, we propose to waive the criterion of preserving accurate spectrum over the Nyquist frequency band, but instead to use for NBL material functions the criterion of maintaining accurate shape of a material function in the time-domain. Justification of the time-domain criterion is provided. Error models are developed for both the accuracy criteria. Increase of the accuracy of filtering algorithms is studied for computing NBL material functions. It is demonstrated that the accuracy of filtering algorithms can be increased by increasing the computing accuracy for bandlimited portions of NBL material functions. Based on this, design of discrete-time filter is proposed by the identification method with employing a pair of bandlimited input and output portions of NBL signal. The proposed design approach is validated by constructing a discrete-time differentiator with using bandlimited portions of the Cauchy pulse and its derivative. The performance of the designed differentiator is evaluated by estimating the mean-square errors for computed derivatives at different sampling frequencies for several smooth NBL test signals, such as the Cauchy pulse, the Hilbert transform of Cauchy pulse, the Gaussian function, as well as for a bandlimited test signal – sinc-function.

Acknowledgements

This work was supported by the European Regional Development Fund under project No. 1.1.1.1/16/A/008 “Development of multi-functional tester for non-destructive quality testing of materials and structures from rigid cellular plastics”.

References:

[1] S. Zhang, L. Li, A. Kumar, *Materials Characterization Techniques*, CRC Press, 2008.
[2] D.C. Jiles, *Introduction to the Principles of Materials Evaluation*, CRC Press, 2007.
[3] V. Shtrauss, Digital Interconversion between Linear Rheologic and Viscoelastic Material Functions, in: *Advances in Engineering Research.* Vol. 3, Ed. V.M. Petrova, Nova Science Publishers, 2012, pp. 91-170.
[4] R.G. Owens, T.N. Phillips, *Computational Rheology*; Imperial College Press, 2002.
[5] J.D. Ferry, *Viscoelastic Properties of Polymers*, J. Wiley and Sons, 1980.
[6] N.W. Tschoegl, *The Phenomenological Theory of Linear Viscoelastic Behavior;* Springer-Verlag, 1989.
[7] N.G. McCrum, B.E. Read, G. Williams, *Anelastic and Dielectric Effects in Polymer Solids;* J. Wiley and Sons, 1967.
[8] L.C.E. Struik, F.R. Schwarzl, Conversion of Dynamic in to Transient Properties and Vice Versa, *Rheol. Acta*, Vol. H. 2, 1969, pp. 134-141.

[9] F.R. Schwarzl, The Numerical Calculation of Storage and Loss Compliance from Creep for Linear Viscoelastic Materials, *Rheol. Acta* Vol. 8, 1969, pp.6-17.

[10] F.R. Schwarzl, On the Interconversion between Viscoelastic Material Functions, *Pure Appl. Chem.*, Vol. 23, 1970, pp. 219-234.

[11] S. Havriliak, S.J. Havriliak, Time to Frequency Domain Transforms, *Polymer*, Vol. 36, 1995, pp. 2675-2680.

[12] S.W. Park, R.A. Schapery, Methods of Interconversion between Linear Viscoelastic Material Functions. Part I – A Numerical Method Based on Prony Series, *Int. J. Solids Struct.*, Vol. 36, 1999, pp. 653–1675.

[13] A.V. Oppenheim, R.V. Schafer, *Discrete-Time Signal Processing*, Prentice-Hall International, 1999.

[14] S.M. Alessio, *Digital Signal Processing and Spectral Analysis for Scientists. Concepts and Applications*, Springer, 2016.

[15] B. Porat, *A Course in Digital Signal Processing*, Wiley, 1997.

[16] V. Shtrauss, Time-domain Aliasing and Anti-Aliasing Effects in Differentiating a Band-Unlimited Signal, *MATEC Web of Conf.*, Vol. 210, 2018, 05005.

[17] V. Shtrauss, Interaction Between Aliasing and Antialiasing Effects in Differentiating Smooth Band-Unlimited Signals, *Int. J. Circ. Syst. Sign. Proc.*, Vol. 13, 2019, pp. 85-91.

[18] W.L. Anderson, Numerical Integration of Related Hankel Transforms of Orders 0 and 1 by Adaptive Digital Filtering, *Geophysics*, Vol. 44, No. 7, 1979, pp. 1287-1305.

[19] D.P. Ghosh, The Application of Linear Filter Theory to the Direct Interpretation of Geoelectrical Resistivity Sounding Measurements, *Geophys. Prosp*., Vol. 19, 1971, pp. 192-217.

[20] F.N. Kong, Evaluation of Fourier Cosine/Sine Transforms Using Exponentially Positioned Samples, *J. Appl.Geophys.*, 2012, Vol. 79, 2012, pp. 46-54.

[21] T.W. Parks, C.S. Burus, *Digital Filter Design*, Wiley, 1987.

[22] S.C.D. Roy, B. Kumar, Digital Differentiators. In: *Handbook of Statistics*, Vol. 10, Eds. N.K. Bose, C.R. Rao, Elsevier, 1993, pp. 159–205.

[23] V. Shtrauss, Functional conversion of signals in the study of relaxation phenomena, *Signal Process*., Vol. 45, 1995, pp. 293-312.

[24] V. Shtrauss, An Approach to Accurate Inversion of Convolution Transforms by FIR Filters, *WSEAS Trans. Signal Process.*, Vol. 10, 2014, pp. 243-254.

[25] V. Shtrauss, A. Kalpinsh, U. Lomanovskis, Splitting Magnitude Response into Real and Imaginary Parts, *MATEC Web Conf*., Vol. 125, 2017, 05004.

[26] V. Shtrauss, A. Kalpinsh, U. Lomanovskis, Separating Magnitude Response into Real and Imaginary Parts by Mellin Convolution Filters, *WSEAS Trans. Signal Process.*, Vol. 13, 2017, pp. 182-189.

[27] V. Shtrauss, A. Kalpinsh, Recovery of Distribution of Relaxation and Retardation Times by Measuring Amplitudes to Multi-Harmonic Excitations, *Proc. 15th WSEAS Int. Conference on Systems*, 2011, pp.112-117.

[28] V. Shtrauss, A. Kalpinsh, Determination of Relaxation and Retardation Spectrum from Modulus of Complex Frequency-Domain Material functions, *WSEAS Trans. Appl. Theor. Mech.*, Vol. 7, No. 1, 2012, pp. 29-38.

[29] J.H. McClellan, T.W. Parks, L.R. Rabiner, A computer program for designing optimum FIR linear phase digital filters, *IEEE Trans. Audio Electroacoust*., Vol. AU-21, No. 6, 1973, pp. 506-526.